Electronic Supplementary Material (ESI) for Physical Chemistry Chemical Physics.

Supplementary Data

Flexibility and Conformation of the Cocaine Aptamer Studied by PELDOR

Claudia M. Grytz[1], Andriy Marko[1], Pavol Cekan[2], Snorri Th. Sigurdsson[2]* and Thomas F. Prisner[1]*

[1] Institute of Physical and Theoretical Chemistry and Center of Biomolecular Magnetic Resonance, Goethe University, 60438 Frankfurt am Main, Max-von-Laue-Str. 9, Hessen, Germany
[2] University of Iceland, Department of Chemistry, Science Institute, Dunhaga 3, 107 Reykjavik, Iceland

* To whom correspondence should be addressed. Email: prisner@chemie.uni-frankfurt.de, snorrisi@hi.is

Table of Contents

1 Similarity between aptamer 1 and 2 in the cocaine-bound state

Figure S1 shows that the average time traces of aptamers **1** and **2** in the presence of cocaine were almost identical and demonstrate that elongation of helix I in aptamer **2** does not influence the structure of the cocaine-bound state. For better comparison, the modulation depths of aptamer **2** were rescaled (Figure S1). The reproducibility of the modulation depth in the PELDOR measurements was within an error of 10% between different samples.

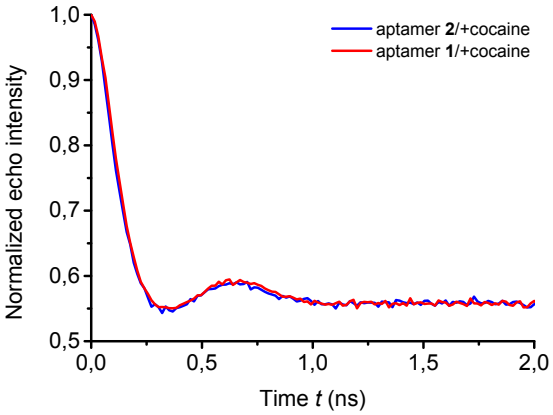

Figure S1. Averaged time traces measured at different frequency offsets of the aptamer **1** (red) and aptamer **2** (blue), both in presence of cocaine. The modulation depth of the blue PELDOR trace for 2.0 µs of the simulation has been adjusted to the red trace to allow a quantitative comparison.

2 PELDOR experiments at X- and Q-band frequencies for aptamer 1 in deuterated solvent

Due to minor angular correlations, reflected in the PELDOR traces of the samples in protonated solvent, measured with a dipolar evolution time of 2.5 µs, one measurement with a frequency offset of 70 MHz at X-band frequencies was recorded for the samples in a deuterated solvent with a dipolar evolution time window of 5 µs. Deuterium modulation was suppressed by averaging 8 spectra of variable τ_1 from 400 to 848 ns in steps τ_1 of 56 ns. To achieve an optimal signal-to-noise ratio, the approximate measurement time was approximately 12 h. All the other experimental parameters were same as the experiments performed on samples in protonated solvent as described in the material and methods section of the main manuscript.

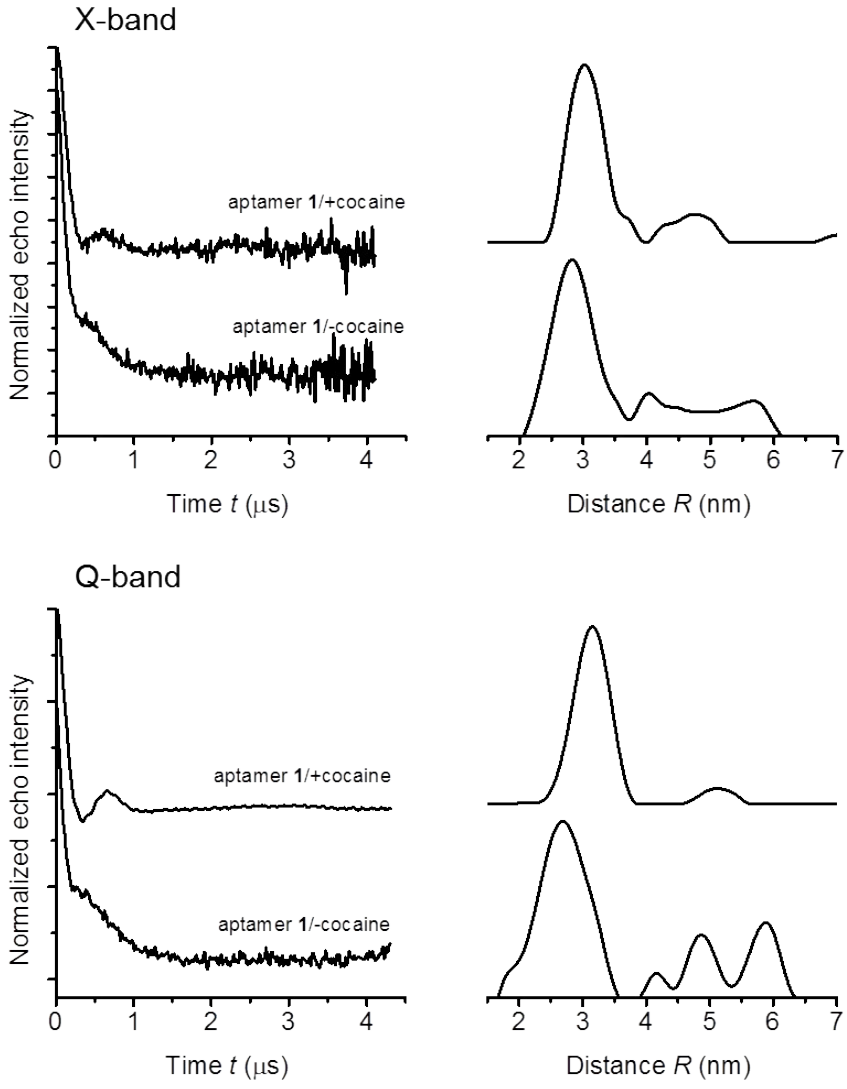

Figure S2. Background-divided time traces of spin-labeled cocaine aptamer **1** in the presence and absence of cocaine in a deuterated solvent at X- and Q-band with a dipolar evolution time t_{max} of 5000 ns. Distance distributions were obtained by Tikhonov regularization.

3 Analysis of PELDOR data

3.1 Analysis of the PELDOR data with respect to distance distributions

3.1.1 *Summary of obtained distances from Tikhonov regularization*

The extracted mean distances by Tikhonov regularization in the distance distribution, shown in Figure 6 are summarized in Table S1.

Table S1. Mean distances obtained from the distance distributions by the Tikhonov regularization of the averaged time traces recorded at X-band frequencies with a dipolar evolution time t_{max} of 2500 ns.

Aptamer	**1**/-cocaine	**1**/+cocaine	**2**/-cocaine	**2**/+cocaine
Mean distance (nm)	2.9	3.2	2.9	3.3

3.2 Analysis of the PELDOR data with respect to orientation dependence

3.2.1 Definition of Euler rotations

The z-x-z convention was used to define the Euler angles. The set of Euler angles $(\alpha_i, \beta_i, \gamma_i)$ of nitroxide *i* (*i*=1 or 2) define the orientation of the nitroxide with respect to the principal axis of the dipolar tensor (x,y,z). The z-x'-z" set of rotation axes was used to define the Euler angles (Figure S3). The transition from (x,y,z) to (x_i,y_i,z_i) is done via two intermediate coordinate systems (x_i',y_i',z_i') and (x_i",y_i",z_i"). The coordinate system (x_i',y_i',z_i') is the result of (x,y,z) rotation about the z-axis through the angle α_i. The coordinate system (x_i",y_i",z_i") is obtained after a rotation of (x_i',y_i',z_i') about the x_i'-axis through the angle β_i. To obtain (x_i,y_i,z_i) the frame (x_i",y_i",z_i") is rotated about the z_i"-axis through the angle γ_i.

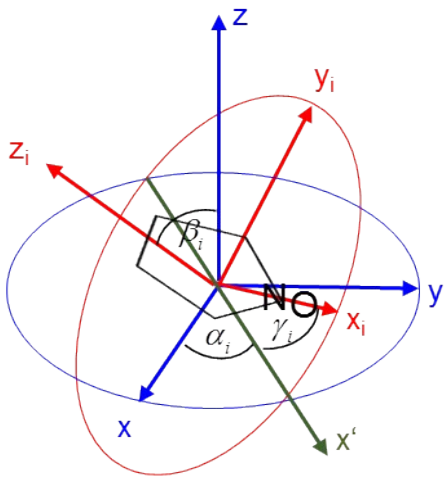

Figure S3. Definition of Euler angles. The (x,y,z) starting coordinate system is shown in blue, the (x_i,y_i,z_i) rotated system is shown in red. The line of nodes (*x'*) is shown in green.

The atom coordinates of the **Ç** spin labelled DNA helices from the pdb-file were transformed into the dipolar coordinate system (x,y,z). The Euler rotation matrixes applied to the atom coordinates are given by

$$D_{1,2}\left(\alpha_{1,2},\beta_{1,2},\gamma_{1,2}\right)=R_z\left(\alpha_{1,2}\right)\cdot R_x\left(\beta_{1,2}\right)\cdot R_z\left(\gamma_{1,2}\right)$$

Both consecutive rotations are required to construct a 3-dimensional biradical structure or rather the relative orientation of the helixes.

3.2.2 PELDOR data simulation

For PELDOR data simulation the following magnetic parameters are required for both nitroxides:

The g-tensor: g_{xx} = 2.0088, g_{yy} = 2.0066, g_{zz} = 2.0027

The A-tensor: A_{xx} = 10 G, A_{yy} = 8 G, A_{zz} = 35 G

The line broadening was set to 4 G. The pulse lengths, flip angles, magnetic field position, pump and probe frequencies were chosen the same as in the experiment. All equations necessary for PELDOR data simulation can be found in the following references (27, 33, 44, 45).

3.2.3 *The X-band PELDOR data of aptamer 1 in the absence of cocaine shows less orientation selection*

In contrast to the cocaine-bound state the experimental X-band PELDOR data shows less orientation selection, no clear offset dependence was observed and indeed a much broader orientation distribution.

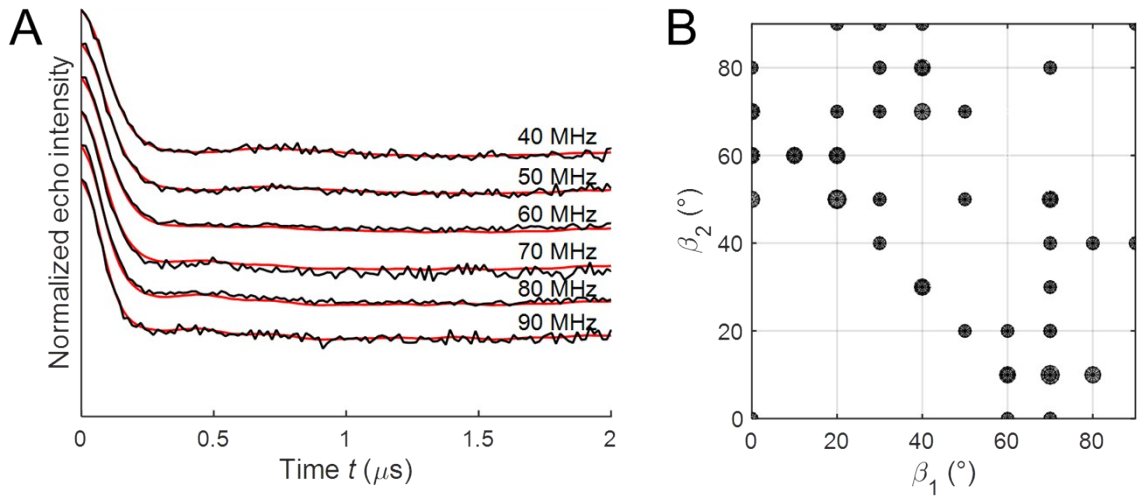

Figure S4. (A) X-band PELDOR signals from the database providing the best fit (red curves) to the experimental PELDOR signals (black curves) with different frequency offsets between probe and pulse from the aptamer with the short helix. Fit and experimental data from the non- bound state. The time traces have been shifted in the direction of the y-axis to aid visual inspection. (B) Angles β_1 and β_2 of the spin label conformers used to fit the experimental 2D PELDOR data set. Each circle represents a spin label conformer and the radius of the circle corresponds to the weight of this conformer in the fit.

3.2.4 Cocaine-bound state

Figure S5 shows the PELDOR data for the cocaine-bound state for aptamer **1**. There is a clear systematic modulation depth dependency, which is reproduced by the PELDOR Database fit.

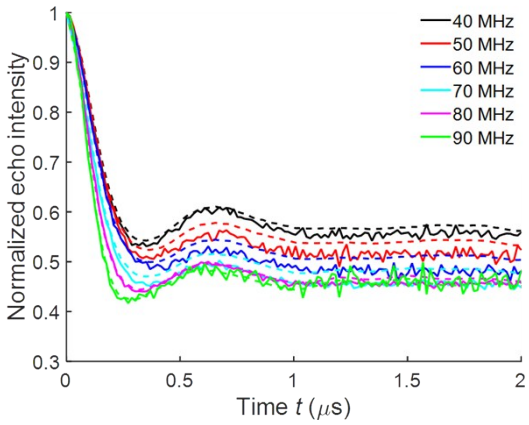

Figure S5. X-band PELDOR signals from the algorithm providing the best fit (dashed lines) to the experimental PELDOR signals with different frequency offsets between probe and pulse from the aptamer with the short helix in the cocaine-bound state. Each color represents a frequency offset.

3.2.4.1 Scaling conditions during the fit procedure

For the cocaine aptamer, the variance in the modulation depth contains the most information about the relative orientation of the rigid **Ç** spin label. However, the modulation depth differences between time traces measured at different frequency offsets could not only result from the relative orientation between two rigid spin labels but also from the experimental setup. Therefore, we tested different ways of scaling the fitted signal to the experimental signal in the y-axis direction during the fit procedure.

There are three ways of scaling the modulation depth: The time traces could be scaled individually, all time traces could be scaled with the same extent or the time traces could not be scaled at all (Figure S6).

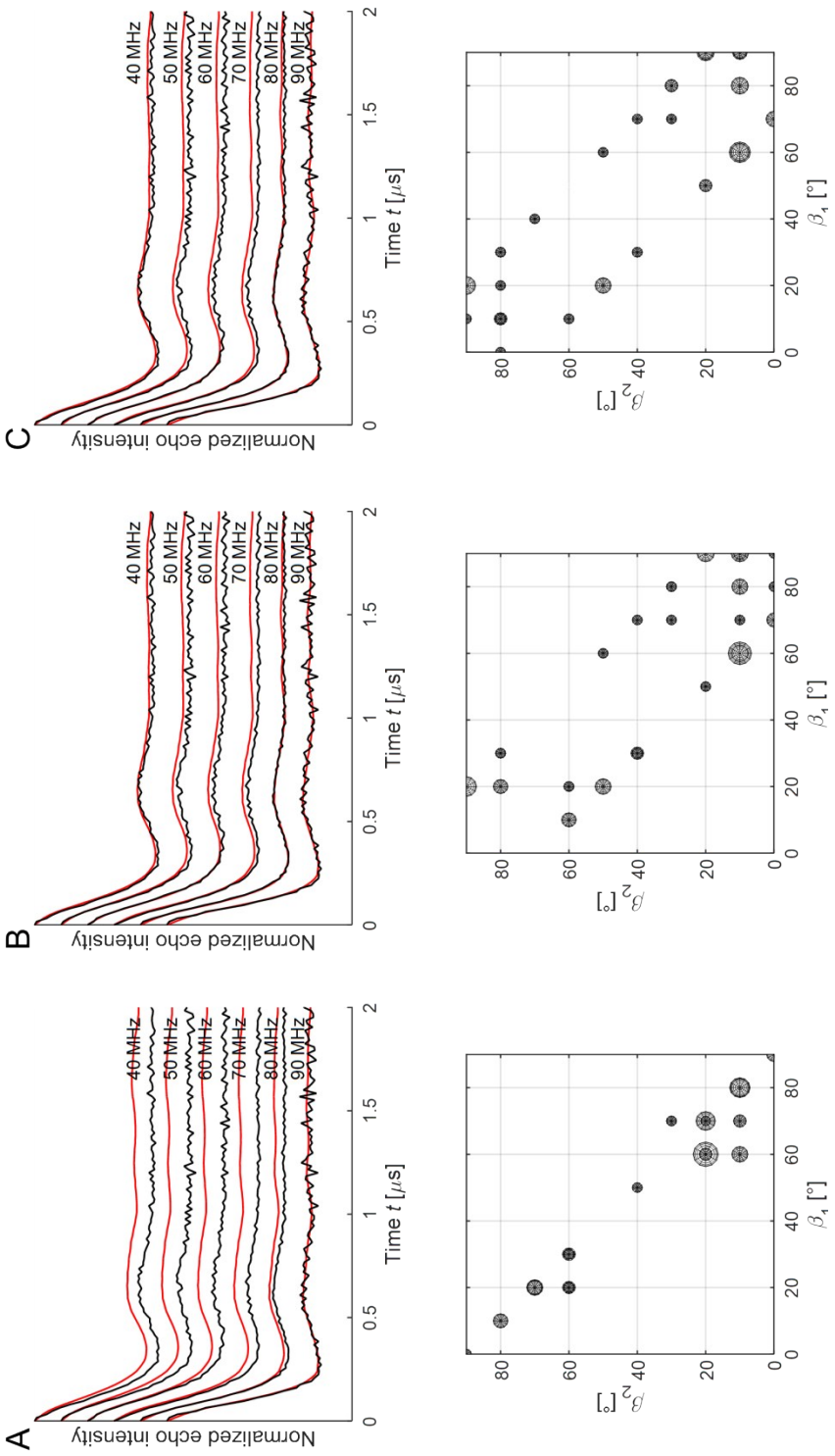

Figure S6. Top: Experimental X-band 2D PELDOR data set for aptamer **1** in the cocaine-bound state (black) and fit by an ensemble of spin label conformers (red) under different scaling conditions. Bottom: Angles β_1 and β_2 of the spin label conformers used to fit the experimental 2D PELDOR data set. Each circle represents a spin label conformer and the radius of the circles corresponds to the weight of this conformer in the fit. (A) During the interactive fitting procedure no scaling was applied. (B) During the fit, the time traces measured at different frequency offsets were scaled individually. (C) During the fit, all time traces were scaled simultaneously.

The fitting algorithm searches in the same conformational space by comparing the geometrical parameters β_1 and β_2 for the fits preformed with different scaling conditions, whereas the fit quality is in all three cases comparably good (Figure S6).

Due to the noise of the experiment, the fitting algorithm would still search for solutions within the same conformational space/ neighborhood. This confirms also that the best strategy for verifying the uniqueness of our solution needs to remove all spin label conformations in the same conformational space. The conformational space of the fit for scaling the modulation depth individually and all in the same extent are nearly identical. This result shows also that the assumption of angle geometrical parameter accuracy is valid when using 10° steps. A further refinement would not yield a better fit. If the magnetic parameters, like the hyperfine coupling and the g-tensor of the system, or an experimental parameter, such as the coupling of the resonator or the pulse lengths during a PELDOR experiment, are known very precisely, a scaling of the modulation depth can be omitted. Usually this is not the case and a scaling of the modulation depth is useful. We prefer to scale the modulation depths with the same extent. Because of the clear systematic modulation depth dependency, we were interested in the relative differences in the modulation depth and not their absolute values.

3.2.4.2 Agreement with the experimental PELDOR data and the obtained structural models

For the simulation, the same statistical weight as in the original database fit result was used (Figure S7). All spin label conformations were taken into account including the remained spin label conformations. The frequency was very well described which confirms that the distance is matched.

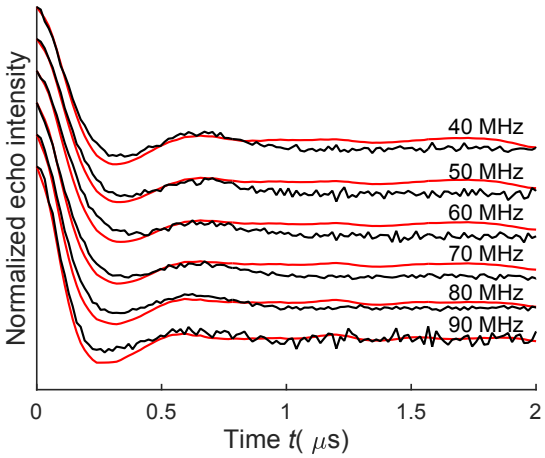

Figure S7. Simulation of the PELDOR time traces (red) resulting from all filtered structural models using the same statistical weight as in the original database fit compared to the experimental data (black).

3.2.4.3 Verifying the uniqueness of the solutions resulting from the fit algorithm

For the fitting approach, no *a priori* structural knowledge of the system is necessary. However, for the interpretation of the geometrical parameters for the predicted spin label conformations, it is indispensable, especially when considering PELDOR experimental data on biological systems.

However, the insufficient orientation selectivity at X-band frequencies has two major consequences for a quantitative analysis of the orientation dependency in PELDOR time traces recorded at this frequency band: On one hand, the symmetry-related solutions introduce some uncertainty into the relative orientation of the spin centers. The equivalence of the PELDOR signals caused by the symmetry has been already analyzed in the work of Abé *et al*. (41). On the other hand, orientation selective PELDOR at X-band frequencies as a method to get from orientation parameters to 3D-bimolecular structures, is not a simple, linear transformation. The geometrical parameters resulting from the PELDOR Database approach might not be unique. Several symmetry-related sets of orientation parameters can provide a qualitatively similar fit to the same experimental PELDOR dataset. A detailed discussion and analysis can be found in the work of Marko *et al*. (29, 33).

There are two strategies to verify the uniqueness of the solutions resulting from a PELDOR Database fit. One would be, to remove all spin label conformations found by the PELDOR Database fit and fit once again with this reduced library. However, the fitting algorithm still searches solutions within the same conformational space/ neighborhood. The angles are in the same order but combined and weighted in a different way. Therefore, the quality of the fit is similar to the fit which uses the whole spin label conformation library (Figure S8). This strategy does also not exclude other possible solutions/ other local minima.

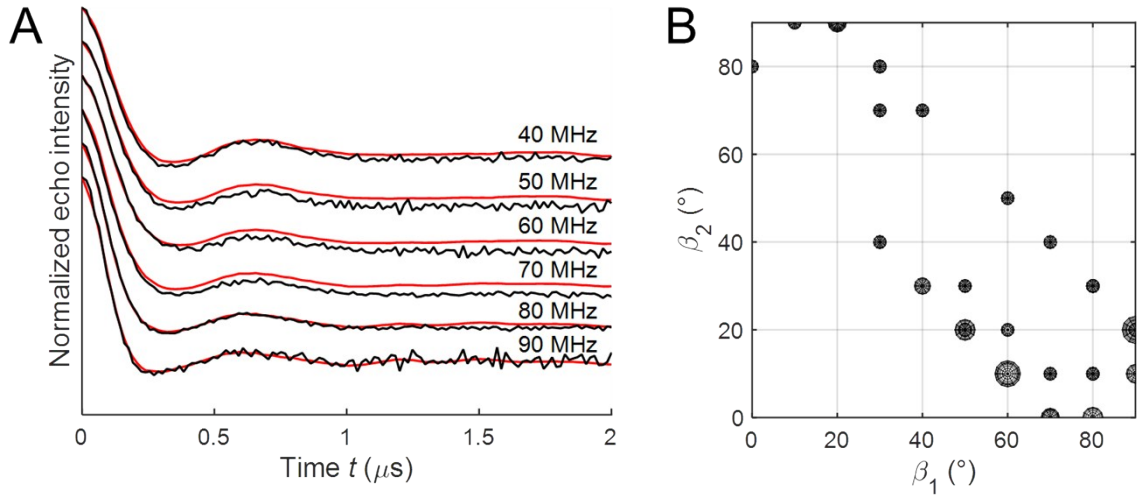

Figure S8. (A) X-band PELDOR signals from the fit algorithm providing the second fit with an ensemble of spin label conformations reduced by the spin label conformers found in the first fit (red curves) to the experimental PELDOR signals (black curves) with different frequency offsets between probe and pulse from the aptamer **1** in the cocaine-bound state. The time traces have been shifted in the direction of the y-axis to aid visual inspection. (B) Angles β_1 and β_2 of the spin label conformers found to fit the experimental 2D PELDOR data set. Each circle represents a spin label conformer and the radius of the circles corresponds to the weight of this spin label conformer in the fit.

As mentioned before, to avoid that the algorithm compensates the removed orientations by selecting similar orientations, we removed a broad area of the spin label conformational space where the solutions from the fit are concentrated (blue squared region in Figure 7).

4 Structural models of aptamer 1 in the cocaine-bound state

Two of the most populated structural models from the conformational ensemble found by the analysis are shown in Figure S9.

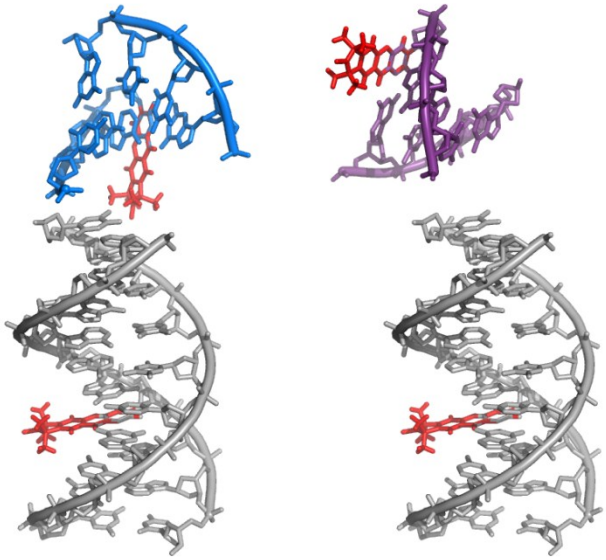

Figure S9. Two representive structural models from the conformational ensemble found by the analysis of aptamer **1** in the cocaine-bound state. The structural models are aligned on the helix II (colored in grey). The twist and bend angles for the left structural model are φ=110°, Ψ=270° and θ=240°, for the right structural model φ=70°, Ψ=10° and θ=130°.

5 Twist and bend angle calculation

For calculating the angles describing a bend of the DNA, we defined two independent coordinate systems for each helix (Figure 6A). Due to the design of the **Ç**, the nitroxide molecular frame of the **Ç** represents the helix frame to which the **Ç** is attached. The out of plane normal of the **Ç** is parallel to the helix axis of the helix where **Ç** is attached.

The bend angle φ is calculated via the scalar product between the z-axes of the **Ç** attached to helix II $\vec{A}_{zz,II}$ and the z-axes of the **Ç** attached to helix III $\vec{A}_{zz,III}$.

$$\varphi[°] = \arccos\left(\vec{A}_{zz,II} \cdot \vec{A}_{zz,III}\right) \cdot \frac{180°}{\pi}$$

The bend angle can be unambiguously calculated from the angles α_1, α_2, β_1 and β_2 in the at X-band frequencies experimentally accessible range.

For the twist angle θ calculation, $\vec{A}_{zz,II}$ is projected to the nitroxide plane, the plane of $\vec{A}_{xx,III}$ and $\vec{A}_{yy,III}$. The sum of the scalar fraction of $\vec{A}_{zz,II}$ in $\vec{A}_{xx,III}$-direction ($antx_{II}$) and the scalar fraction in $\vec{A}_{yy,III}$ direction ($anty_{II}$) results in the vector.

$$\vec{A}_{zz,III}' = \left(\vec{A}_{xx,II} \cdot \vec{A}_{zz,III}\right) \cdot \vec{A}_{xx,II} + \left(\vec{A}_{yy,II} \cdot \vec{A}_{zz,III}\right) \cdot \vec{A}_{yy,II}$$
$$\vec{A}_{zz,III}' = antx_{II} \cdot \vec{A}_{xx,II} + anty_{II} \cdot \vec{A}_{yy,II}$$

For angle calculation within the interval [π, -π], $\vec{A}_{zz,III}'$ was defined as a complex number $A_{zz,III}' = antx_{II} + i \cdot anty_{II}$. The twist angle is then the phase angle of

$\theta[°] = \text{atan2}\left(anty_{II}, antx_{II}\right) \cdot \frac{180°}{\pi}$ (four-quadrant arctangent see Matlab documentation atan2) to have the angles within the interval [0, 2π], θ was increased by 2π if θ was negative. The twist angle Ψ was calculated in an analog manner.

The weighted mean bend angle and its standard deviation are calculated by

$$\bar{\varphi} = \frac{\sum_{i=1}^{N} \varphi_i \cdot w_i}{\sum_{i=1}^{N} w_i} \text{ and } \sigma_{\bar{\varphi}} = \sqrt{\frac{\sum_{i=1}^{N} \left(\varphi_i - \bar{\varphi}\right)^2 \cdot w_i}{\sum_{i=1}^{N} w_i}}$$

6 Original experimental PELDOR time traces

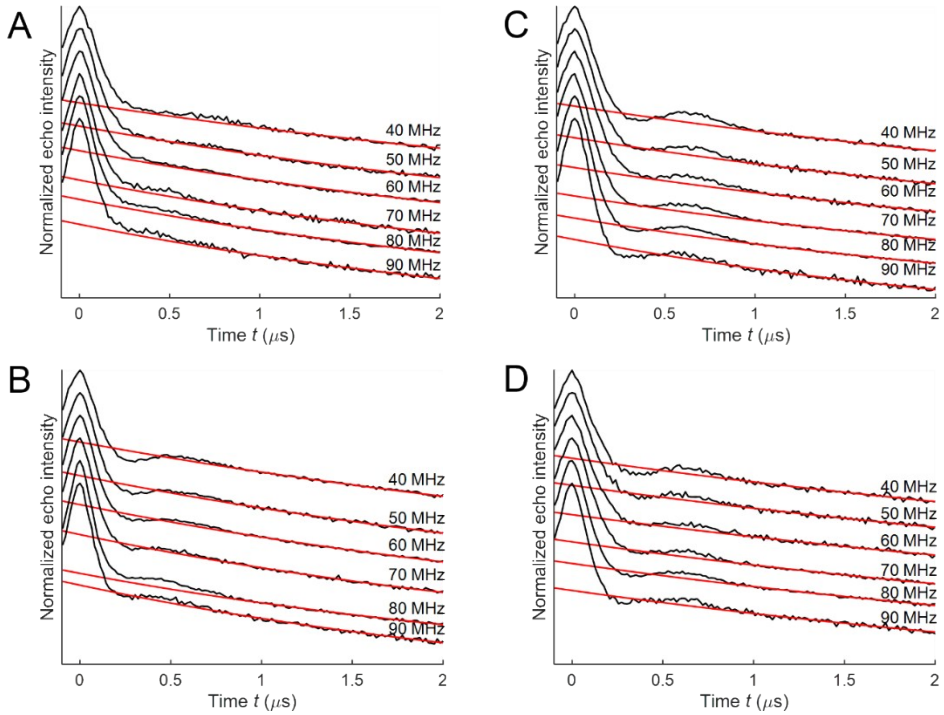

Figure S10. Experimental PELDOR time traces measured at frequency offsets $\Delta\nu$ from 40 to 90 MHz at X-band for spin-labeled aptamers **1** (A), (B) and **2** (C), (D) in the absence and presence of cocaine, respectively.

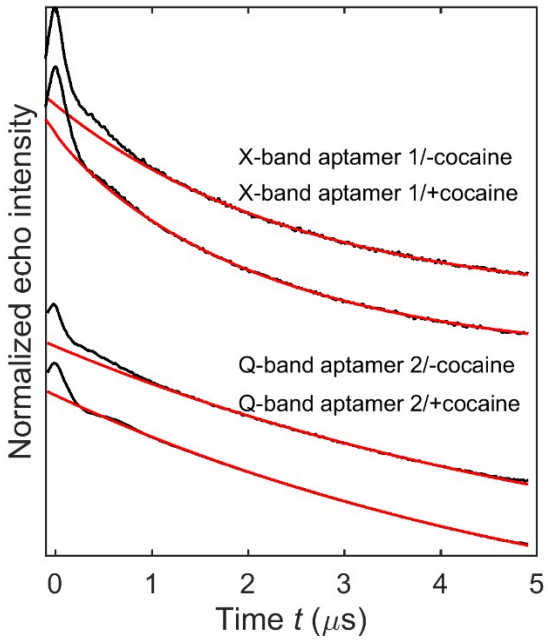

Figure S11. Experimental time traces of spin-labeled cocaine aptamer **1** in the presence and absence of cocaine in a deuterated solvent at X- and Q-band with a dipolar evolution time t_{max} of 5000 ns. Distance distributions were obtained by Tikhonov regularization.